energies

MDPI

Article

A Bilevel Programming Framework for Demand Response Incentive Design with Non-Intrusive Load Monitoring-Based Flexibility Estimation

Ye Ding [1], Kai Zhou [1,2,*], Xiuming He [3] and Yuan Sun [1,*]

[1] School of Mechanical and Electrical Engineering, Soochow University, Suzhou 215000, China; 20254229039@stu.suda.edu.cn
[2] Collaborative Innovation Center of Industrial Energy-Saving and Power Quality Control, Anhui University, Hefei 230601, China
[3] Suzhou Electrical Apparatus Science Research Institute Co., Ltd., Suzhou 215000, China; jhtechnical@126.com
* Correspondence: kzhou@suda.edu.cn (K.Z.); yuansun@suda.edu.cn (Y.S.)

Abstract

Demand response (DR) plays a key role in enhancing power system flexibility under increasing renewable penetration, yet most existing approaches rely on aggregate demand models that fail to capture appliance-level heterogeneity. A bilevel programming framework for DR incentive design incorporating non-intrusive load monitoring (NILM)-based flexibility estimation is proposed. A conditional factorial hidden Markov model (CFHMM) is used to disaggregate smart meter data and recover appliance-level consumption patterns, which are then mapped to willingness-to-accept (WTA) values to construct device-informed DR potential functions. These estimates are embedded in a bilevel optimization model, where a retailer determines optimal incentives while accounting for the endogenous impact of demand response on locational marginal prices through market clearing. The model is reformulated as a single-level mixed-integer linear program using Karush–Kuhn–Tucker (KKT) conditions. Case studies using real-world data and the IEEE test system show that the proposed framework produces more effective incentive strategies than aggregate DR modeling, leading to improved DR utilization and higher retailer profitability.

Keywords: demandresponse; non-intrusive load monitoring; bilevel programming; mixed integer linear programming

Check for updates

Academic Editor: Seung-Hoon Yoo

Received: 11 May 2026
Revised: 5 June 2026
Accepted: 9 June 2026
Published: 12 June 2026

Copyright: © 2026 by the authors. Licensee MDPI, Basel, Switzerland. This article is an open access article distributed under the terms and conditions of the Creative Commons Attribution (CC BY) license.

1. Introduction

As electrification and renewable generation increase, net-load uncertainty emerges and significantly affects secure power system operations. This changes the temporal and spatial characteristics of electricity supply and increases the need for flexible demand-side resources. At the consumer level, distributed renewables and behind-the-meter energy storage are reshaping consumption patterns from passive load profiles into increasingly flexible and controllable resources. However, without accurate prediction and appropriate coordination, the aggregated response of household flexible resources may be mischaracterized and potentially undesirable, such as rebound peaks, sharper ramping, voltage deviations, and additional system stress [1]. Accordingly, demand response (DR) has become critical for modern power system flexibility, which is a proven tool to maintain system reliability, lower procurement costs, and reduce emissions through the temporal shifting or curtailment of electricity consumption during periods of system stress [2–4].

DR programs are typically implemented by utilities or electricity retailers whose primary objective is to maximize economic returns [5,6]. Among various DR mechanisms, price-based programs constitute a major category. Retailers design dynamic pricing or incentive schemes to influence consumer electricity consumption patterns. Through these strategies, electricity demand can be curtailed or shifted in time to better align with system conditions and market prices. Early work primarily focused on characterizing consumer response through price elasticity models and aggregate demand functions [2,5]. While these approaches provide tractable representations of demand behavior, they often rely on simplified assumptions that do not capture the heterogeneity and operational constraints of individual loads.

DR not only changes electricity consumption but also affects electricity market outcomes. In wholesale markets, load changes influence locational marginal prices (LMPs) [7], which in turn affect the economic incentives for both retailers and consumers. This creates a coupled interaction between demand behavior and electricity market clearing. To capture this interaction, bilevel optimization has emerged as a powerful tool, where upper-level decision-makers (e.g., retailers or aggregators) design pricing or incentive schemes, and lower-level agents (e.g., consumers or markets) respond optimally.

A substantial body of literature has applied bilevel programming to model strategic interactions in electricity markets [8,9]. Foundational works such as [10,11] formulate market-clearing processes as lower-level problems, enabling the analysis of price endogeneity and strategic behavior. Extensions of this framework have incorporated demand response participants, modeling retailers or aggregators as leaders who influence consumption through dynamic pricing [12,13]. More recent studies further account for uncertainty and heterogeneity using stochastic or distributionally robust bilevel formulations [9,14]. These models provide a rigorous representation of market-coupled DR but typically rely on stylized assumptions about customer behavior. However, the flexible demand available to the retailer is often represented by aggregate elasticity, representative response functions, or exogenously specified DR blocks. Such representations do not explicitly identify which appliances provide flexibility, when this flexibility is available, or how different end uses imply different compensation requirements.

A key challenge in applying such models to incentive-based DR is how to represent customer compensation requirements. In this context, willingness to accept (WTA) provides an economically interpretable measure of the minimum compensation required for customers to curtail, shift, or otherwise modify electricity consumption. Recent studies on WTA estimation in residential DR mainly adopt stated-preference methods within a random-utility framework. Typical approaches include choice experiments combined with random-parameter logit, mixed logit, latent class analysis, hierarchical Bayes estimation, or direct specification in WTA space [15–17]. These methods provide useful economic interpretations of customer compensation requirements, but they usually estimate WTA at the customer or program-attribute level and do not directly show how appliance-level flexibility can be integrated into system-level DR optimization.

In addition, consumer loads are strongly affected by local weather conditions. Temperature, humidity, solar irradiance, and seasonal variation directly influence the operation of weather-sensitive end uses, especially heating, ventilation, and air-conditioning systems, water heaters, and refrigeration loads. As a result, consumers with similar appliance ownership may exhibit substantially different load profiles in different climate regions. This weather-related heterogeneity limits the transferability of aggregate demand models and customer-level WTA estimates across regions. Therefore, DR incentive design should account for the temporal, spatial, and appliance-level variability of consumer load rather than relying only on aggregate load representations.

To address the limitations of traditional elasticity-based models, an emerging line of research has explored data-driven approaches to characterize consumer behavior. Machine learning techniques, including regression models, deep neural networks, and reinforcement learning, have been employed to predict load responses and optimize DR strategies [18,19]. These methods can capture complex, nonlinear relationships between prices and consumption, improving predictive accuracy compared to parametric models. In parallel, inverse optimization and behavioral modeling approaches have been proposed to infer consumer preferences and utility functions directly from observed data [20]. Such methods aim to bridge the gap between purely predictive models and optimization-based decision frameworks by recovering the underlying economic structure of consumer choices. Despite these advances, most data-driven DR models remain limited in two key aspects. First, they often treat demand as an aggregate signal, without explicitly accounting for the physical characteristics and operational constraints of individual appliances. Second, many approaches focus on response prediction or local control, rather than converting appliance-level flexibility into economic supply curves that can be used for retailer-level incentive planning. As a result, the link between data-driven flexibility estimation and market-aware DR incentive design remains incomplete.

Non-intrusive load monitoring (NILM) offers a promising solution to extract appliance-level information from aggregate electricity consumption data. NILM aims to disaggregate aggregate electricity consumption measured at a single point, such as a smart meter, into appliance-level usage signals. The concept of NILM was first introduced by Hart [21] and has since attracted significant research attention. Existing studies have investigated various NILM techniques, including optimization-based methods, stochastic process models, and neural network approaches. From the perspective of data resolution, algorithms have been developed for both low-frequency smart meter data [22] and high-frequency measurements [23]. Most NILM studies primarily focus on improving disaggregation accuracy and robustness, such as transfer-learning-based methods [24]. However, the potential of NILM outputs to support demand response program design has not been fully explored. Importantly, DR applications do not necessarily require precise identification of every appliance; rather, NILM-derived usage patterns can reveal characteristics of flexible loads and DR potential that support more accurate estimation of customer responsiveness.

Several studies have investigated the use of NILM for estimating load flexibility and supporting demand response applications. They typically focus on identifying flexible appliances, such as thermostatically controlled loads, and optimizing their operation to reduce energy costs or provide grid services. For example, Ref. [25] proposes a contrastive sequence-to-point learning method for disaggregating flexible thermostatically controlled loads and estimating DR potential, while [26] develops an unsupervised NILM framework to estimate DR flexibility and minimize daily electricity bills. Ref. [27] designs a building-level NILM system with integrated hardware and software to support DR programs, although it does not investigate optimal control strategies to realize the full DR potential. These studies show that NILM can reveal appliance-level flexibility hidden in aggregate meter data. However, most existing NILM-based DR studies operate at the device, household, or building level and assume exogenous price or control signals. They rarely translate NILM outputs into WTA-based DR supply curves, and they do not generally embed such curves into retailer-level incentive optimization with endogenous market-price feedback.

The above studies can be grouped into two related but largely separate streams. Market-oriented DR models capture incentive design and price feedback but usually simplify demand flexibility. In these studies, customer responses to incentives are modeled as WTA or data-driven methods but often do not resolve appliance-level operational constraints. As a result, the resulting DR potential may either overestimate or underestimate

the flexibility that can realistically be activated at a given time. On the other hand, NILM studies recover appliance-level usage patterns from aggregate meter data. Although such information is highly relevant to DR flexibility estimation, NILM outputs are rarely embedded into retailer-level or market-coupled incentive optimization. In particular, limited attention has been paid to translating NILM-derived appliance profiles into actionable economic models for DR program planning, especially under market-clearing interactions. Therefore, an important gap exists between appliance-level flexibility estimation and market-level DR incentive design. This gap limits the ability of retailers to design incentives that reflect both the temporal availability of flexible appliances and their heterogeneous willingness to accept compensation.

To bridge these gaps, a bilevel programming framework for demand response incentive design incorporating NILM-based flexibility estimation is proposed. Specifically, NILM outputs from smart meter data are utilized to infer device-level usage characteristics and estimate the WTA of electricity loads. These estimates are then incorporated into a bilevel optimization framework in which the retailer determines incentive schemes and the load changes are reflected in the resulting LMPs. By linking NILM-derived information with DR incentive design, the proposed framework enables more accurate modeling of customer behavior and improves the effectiveness of demand response programs.

The main contributions of this paper are summarized as follows:

- An NILM-informed framework is proposed for estimating demand response flexibility, in which disaggregated appliance-level consumption profiles are mapped to time-varying, stepwise DR supply curves using appliance-specific WTA thresholds.
- A retailer–independent system operator (ISO) bilevel programming model is formulated for DR incentive design, in which the retailer optimizes incentive prices and procured DR quantities while accounting for the endogenous impact of demand response on market-clearing outcomes and locational marginal prices.
- The resulting bilevel problem is reformulated as a single-level mixed-integer linear program by applying KKT conditions to the ISO market-clearing problem and linearizing the complementarity and bilinear terms, thereby enabling tractable computation of optimal incentive strategies.

2. Framework for the NILM-Based Incentive Design

A demand response incentive optimization problem for utilities or electricity retailers is defined. The retailer serves residential consumers located within a centralized electricity system. To account for the interaction between retailer incentive decisions and electricity market outcomes, the problem is formulated as a bilevel optimization model, in which the upper level is retailer profit maximization and the lower level is ISO market clearing.

In this setting, households are connected to a retailer and participate indirectly in the electricity market through incentive-based demand response programs. Although neural-network-based methods have been widely used for load forecasting, NILM, and demand response prediction, such methods alone do not explicitly model incentive compatibility, willingness-to-accept compensation, or market-clearing feedback. Therefore, this study uses NILM not as a standalone prediction tool, but as a means of extracting appliance-level flexibility information for market-oriented incentive optimization. The retailer observes aggregate household smart-meter data, estimates the available flexible demand, and determines incentive prices to activate demand response. The activated demand response then changes the net load submitted to the market, which in turn affects the ISO market-clearing results and locational marginal prices. Therefore, the problem consists of three coupled components: extracting appliance-level flexibility from aggregate household consumption, converting this flexibility into a willingness-to-accept-based demand response supply

curve, and optimizing retailer incentives while accounting for market-clearing feedback. Figure 1 illustrates this overall workflow. The left part of the figure represents household smart-meter data collection; the middle part represents NILM-based disaggregation and DR potential extraction; and the right part represents the retailer–ISO bilevel optimization and its bilevel optimization formulation.

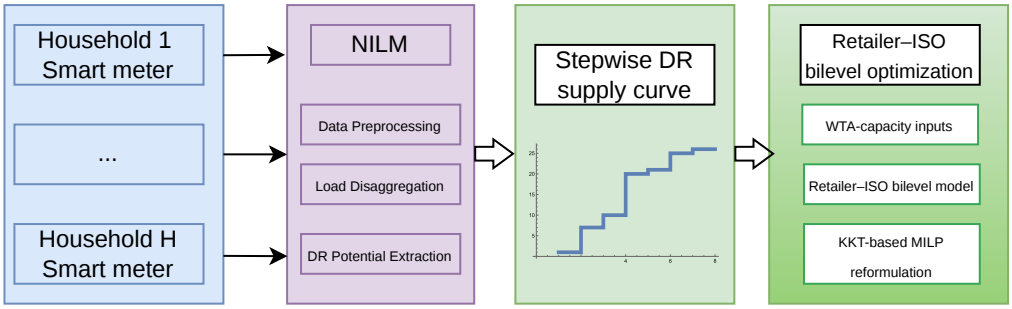


Figure 1. Overall framework of the proposed NILM-based DR incentive design method.

2.1. Nilm Algorithm

Since smart meter data are typically collected at low sampling rates (1 Hz or less), the Conditional Factorial Hidden Markov Model (CFHMM) is used to disaggregate smart meter data for each household [28]. Stable-state features are used as they can be more readily obtained from smart meters and no additional equipment is required. Selected features include time of day and day of week.

2.1.1. Model

Each appliance is assumed to have two states (on and off) and is modeled as a Markov chain. Note that the binary state represents the activation state of an appliance, rather than a fixed deterministic power level. The measured aggregate power remains a continuous variable modeled through the Gaussian observation equation described below. The appliance states evolve independently and combine additively to produce the observed aggregate power. For appliance $e \in \{1, \ldots, E\}$ and time $t \in \{1, \ldots, T\}$, let $s_{e,t}$ be the state of appliance e, and $c_{k,t}$ be the external features that $s_{e,t+1}$ depends on.

The initial probability is

$$\pi_{e,s_{e,1}} = P(s_{e,1} = k), \quad k \in \{0, 1\} \tag{1}$$

where $P(\cdot)$ is the probability of a random variable.

To describe the dependence of appliances' states on conditions $c_{k,t}$, define feature factors:

$$f_e(s_{e,t}, c_{k,t-1}) = P(c_{k,t-1} = l | s_{e,t} = j) \tag{2}$$

Note that it is formulated backwards in time; that is, the condition at time $t-1$ is dependent on the appliance state at time t. This formulation allows the transition probability to be constructed as a product of simple, normalized pairwise terms, which facilitates learning using the Expectation-Maximization (EM) algorithm.

The cross-appliance factors are

$$m_e(s_{e,t}, s_{r,t-1}) = P(s_{r,t-1} = l | s_{e,t} = j) \tag{3}$$

During the on state, the total real power follows a normal distribution [28]. Let μ_e be the mean real power $p_{e,t}$ when appliance e is on, and let σ^2 be the variance for all e; then, p_t follows a normal distribution:

$$p_t|\boldsymbol{s}_t \sim b_{\boldsymbol{s}_t}(p_t) = \mathcal{N}(\textstyle\sum_{e=1}^{E} \mu_e s_{e,t}, \sigma^2) \tag{4}$$

where E is the total number of appliances, and $\boldsymbol{s}_t = [s_{1,t}, s_{2,t}, \ldots, s_{E,t}]$ denotes the vector of all appliance states at time t. Throughout the paper, bold symbols are used to represent vectors of random variables.

The transition from $s_{e,t-1}$ to $s_{e,t}$ conditional on $c_{k,t-1}$ and cross-appliance interaction effects is

$$P(\boldsymbol{s}_t|\boldsymbol{s}_{t-1}, c_{t-1}) \propto \prod_{e=1}^{E} \phi_e(s_{e,t}, \boldsymbol{s}_{t-1}, c_{t-1}) \tag{5}$$

where

$$\phi_e(s_{e,t}, \boldsymbol{s}_{t-1}, c_{t-1}) = \prod_k f_e(s_{e,t}, c_{k,t-1}) \cdot \prod_{r \neq e} m_e(s_{e,t}, s_{r,t-1}) \tag{6}$$

The proportionality constant ensures normalization.

Each Markov chain in CFHMM has transitions conditional on other chains and external features at t. The joint distribution remains additive-Gaussian. Thus, the joint distribution of the real power $\boldsymbol{p}$ and the appliance state sequence $\boldsymbol{s}$ is

$$P(\boldsymbol{p}, \boldsymbol{s}|\Theta) = \prod_{e=1}^{E} \pi_{e,s_{e,1}} \prod_{t=1}^{T} b_{\boldsymbol{s}_t}(p_t) \prod_{t=2}^{T} P(\boldsymbol{s}_t|\boldsymbol{s}_{t-1}, c_{t-1}) \tag{7}$$

where $\Theta = \{\pi_e, \mu_e, \sigma^2, f_e, m_e\}$, $\boldsymbol{s} = \{s_{e,t}\}$, $\quad e \in E, t \in T$.

2.1.2. Learning

The parameter set Θ is estimated from aggregate smart meter data $\boldsymbol{p} = \{p_t\}_{t=1}^{T}$. Since appliance states $\boldsymbol{s} = \{s_{e,t}\}$ are not directly observable, parameter estimation is formulated as a latent-variable learning problem. Specifically, the Expectation-Maximization (EM) algorithm is employed [29] to maximize the marginal likelihood:

$$\max_{\Theta} P(\boldsymbol{p}|\Theta) = \sum_{\boldsymbol{s}} P(\boldsymbol{p}, \boldsymbol{s}|\Theta) \tag{8}$$

In the E-step, the posterior distribution over appliance states $P(\boldsymbol{s}|\boldsymbol{p}, \Theta)$ is computed, providing the expected activation probabilities and transition statistics. In the M-step, parameters are updated by maximizing the expected complete-data log-likelihood. This yields closed-form updates for the initial state probabilities, appliance power levels, and noise variance, while feature-dependent and cross-appliance transition factors are estimated from conditional expectations. The EM iterations continue until convergence.

2.1.3. Prediction

Given the learned parameters Θ, the hidden sequences are estimated by

$$\boldsymbol{s}^* = \arg\max_{\boldsymbol{s}} P(\boldsymbol{s}|\boldsymbol{p}, \Theta) \tag{9}$$

Exact inference is intractable due to the factorial and coupled structure of the model. Therefore, the simulated annealing method is used to approximate the optimal state sequence. Appliance-level power is then reconstructed as

$$\hat{p}_{e,t} = \mu_e P(s_{e,t} = 1 | \boldsymbol{s}, \Theta) \tag{10}$$

The resulting disaggregated load profiles are used to derive demand response flexibility.

2.2. Extract DR Potential from NILM Result

The NILM output provides appliance-level power consumption $p_{e,t}^{(b)}$ for each appliance e, household b and time t. To utilize this information for DR modeling, these disaggregated load profiles are transformed into a WTA-responsive flexibility representation.

Appliances are grouped into categories according to their controllability and typical DR actions, as shown in Table 1, such as heating, ventilation, and air conditioning (HVAC) adjustment, electric vehicle (EV) charging shift, or appliance deferral. For each household b, the flexible load in category m is defined as

$$h_{t,m}^{(b)} = \sum_{e \in \text{category } m} p_{e,t}^{(b)} \tag{11}$$

Aggregating across all households yields the total flexible capacity:

$$h_{t,m} = \sum_{b=1}^{B} h_{t,m}^{(b)} \tag{12}$$

This aggregation produces a time-varying estimate of available flexibility for each appliance category.

Table 1. Willingness-to-accept prices of different appliances.

Appliance	Typical DR Action	WTA
Base load	No action	v_5
HVAC	Thermostat setback	v_4
EV charging	Shift or throttle	v_3
Washer/Dryer	Delay cycle	v_2
Dishwasher	Delay start	v_1
Lighting & misc. plug loads	Turn off/dim	v_0

Each appliance category m is associated with a willingness-to-accept (WTA) threshold v_m, representing the minimum compensation required for users to curtail or shift consumption. Categories with higher comfort impact or operational constraints are assigned higher WTA values, while more flexible loads have lower thresholds. Inflexible loads are assigned $v_5 = \infty$, ensuring that they are not activated.

Using the aggregated flexibility $h_{t,m}$ and corresponding WTA values v_m, a stepwise DR supply function is constructed that maps incentive levels to available curtailable load.

For a given incentive price τ_t, the appliance-informed DR supply quantity is

$$Q_t^{\text{DR}}(\tau_t) = \sum_{m: v_m \leq \tau_t} h_{t,m} \tag{13}$$

This formulation implies that load segments are activated in order of increasing WTA, such that lower-cost flexibility is utilized before higher-cost resources.

The resulting stepwise function represents a price–quantity supply curve of demand response, where each segment corresponds to a category of flexible loads. This structure preserves both heterogeneity across appliance types (through different WTA levels) and tem-

poral variability (through time-dependent $h_{t,m}$). This appliance-informed DR representation serves as the input to the upper-level incentive optimization problem.

2.3. Bilevel Programming for DR Incentive Strategy

To determine optimal demand response incentives, the interaction between the retailer and the wholesale electricity market is modeled under a bilevel decision framework. The retailer determines the incentive signal and the amount of DR flexibility to be activated, while the independent system operator (ISO) determines the market-clearing outcome under network constraints.

The DR potential derived in the previous section is represented by a stepwise price–quantity supply curve. For each time period, the available curtailable load is characterized by segment-wise willingness-to-accept thresholds and corresponding flexible capacities. Accordingly, DR segments are activated according to the offered incentive level, and lower-threshold segments are selected before higher-threshold segments.

2.3.1. Upper Problem

The retailer determines the incentive price τ_t and procured DR capacity $q_{n,t}$ at bus n and time t. Suppose the retail price is π_t; the objective of the retailer is to maximize the profit over the scheduling periods:

$$\max_{\tau_t, \boldsymbol{q}} \sum_{t \in \mathcal{T}} \sum_{n \in \mathcal{N}^{\mathrm{DR}}} (\pi_t - \lambda_{n,t}) y_{n,t} - \tau_t q_{n,t} \tag{14}$$

where $y_{n,t}$ denotes the post-DR served retail demand at bus n and time t, and $q_{n,t}$ denotes the activated DR quantity. The first term represents the retailer's net revenue from serving the remaining load after DR, while the second term represents the incentive payment for activated load curtailment over all buses in the retailer's footprint.

The DR response is modeled by a segment function. Each segment corresponds to a DR resource with the same WTA and those with lower WTA are activated first.

$$q_{n,t} = \sum_{m \in \mathcal{M}} b_{n,t,m}, \quad \forall n, t \tag{15}$$

$$0 \le b_{n,t,m} \le h_{n,t,m} z_{n,t,m}, \quad \forall n, t, m \tag{16}$$

$$z_{n,t,m+1} \le z_{n,t,m}, \quad \forall n, t, m = 1, \ldots, |\mathcal{M}| - 1 \tag{17}$$

$$\tau_t + (v_m - \underline{\tau})(1 - z_{n,t,m}) \ge v_m, \quad \forall n, t, m \tag{18}$$

$$z_{n,t,m} \in \{0, 1\} \quad \forall n, t, m. \tag{19}$$

Equation (15) shows that the total activated DR quantity $q_{n,t}$ is the sum of the activated segment quantities $b_{n,t,m}$. Equation (16) limits each segment by its available capacity $h_{n,t,m}$. Equation (17) ensures that lower-WTA segments are activated before higher-WTA segments. Equation (18) ensures that segment m can be activated only when the offered incentive τ_t reaches its WTA threshold v_m. If $z_{n,t,m} = 1$, then $\tau_t \ge v_m$; otherwise, the constraint reduces to $\tau_t \ge \underline{\tau}$, where $\underline{\tau}$ denotes the lower bound of the incentive price. Therefore, only those DR segments whose WTA thresholds are covered by the offered incentive can be activated. The binary variable $z_{n,t,m}$ indicates whether segment m at bus n and time t is activated.

The actual load after DR is

$$y_{n,t} = d_{n,t} - q_{n,t}, \quad n \in \mathcal{N}^{\mathrm{DR}}, t \in \mathcal{T}. \tag{20}$$

And the incentive price is bounded by

$$\underline{\tau} \leq \tau_t \leq \bar{\tau}, \quad t \in \mathcal{T}. \tag{21}$$

The total activated DR quantity over all DR buses at time t is defined as q_t. The intertemporal constraints on DR activation are

$$q_t = \sum_{n \in \mathcal{N}^{\mathrm{DR}}} q_{n,t}, \tag{22}$$

$$q_t - q_{t-1} \leq R^{\mathrm{up}}, \tag{23}$$

$$q_{t-1} - q_t \leq R^{\mathrm{down}}, \quad t \in \mathcal{T} \setminus \{1\}. \tag{24}$$

where q_t denotes the total activated DR quantity aggregated over all DR buses at time t, and R^{up} and R^{down} denote the upward and downward ramp limits of total DR activation, respectively. The cumulative DR energy constraint is imposed to represent the finite intertemporal availability of flexible demand, preventing unrealistically persistent activation of demand response across the scheduling horizon. That is

$$\sum_{t \in \mathcal{T}, n \in \mathcal{N}^{\mathrm{DR}}} q_{n,t} \leq E^{\mathrm{DR}}_{\max} \tag{25}$$

2.3.2. Lower Problem

In the upper problem, LMP $\lambda_{n,t}$ at bus n is determined by the market clearing procedure. When LMP is greater than the compensation required to induce end-user flexibility, the retailer would activate the DR program. In return, as the load is altered by the DR, the LMP would change accordingly. This process is modeled through an optimal-power-flow-based market-clearing model.

The ISO minimizes the overall system cost at time step t through

$$\min_{g,r,\theta,f} \quad \sum_{i \in \mathcal{G}} C_i(g_{i,t}) + C^r_i(r_{i,t}) \tag{26}$$

subject to

$$\sum_{i \in \mathcal{G}(n)} g_{i,t} - \sum_{\ell \in \delta(n)} f_{\ell,t} = d_{n,t} - q_{n,t}, \quad \forall n, \tag{27}$$

$$f_{\ell,t} = b_\ell \sum_{n \in \mathcal{N}} A_{\ell n}\, \theta_{n,t}, \quad \forall \ell, \tag{28}$$

$$-F^{\max}_\ell \leq f_{\ell,t} \leq F^{\max}_\ell, \quad \forall \ell, \tag{29}$$

$$G^{\min}_i \leq g_{i,t} \leq G^{\max}_i, \quad \forall i, \tag{30}$$

$$\sum_{i \in \mathcal{G}} r_{i,t} \geq R^{\mathrm{req}}_t, \tag{31}$$

$$0 \leq r_{i,t} \leq G^{max}_i - g_{i,t}, \quad \forall i \tag{32}$$

$$\theta_{n_0,t} = 0, \tag{33}$$

where (27) is the nodal power balance constraint; $\lambda_{n,t}$ is the dual variable of (27), which is the LMP used in (14); Equation (28) is the DC power flow equation. $A_{\ell n}$ is the incidence matrix; for each line ℓ with "from" bus n_f and "to" bus n_t, $A_{\ell n} = 1$ if $n = n_f$ and $A_{\ell n} = -1$ if $n = n_t$; otherwise, $A_{\ell n} = 0$. Equation (29) is the line flow limit; Equation (30) is the generator output limit; Equations (31) and (32) are the reserve requirements.

In summary, the main modeling procedure is shown in Figure 2. The procedure starts from smart-meter data collection and data cleaning. A CFHMM model is trained

using historical smart-meter data and then used for NILM-based load disaggregation. The disaggregated minute-level appliance profiles are aggregated into hourly appliance-level profiles, which are further converted into flexibility estimates and WTA-based DR supply curves. Finally, these inputs are incorporated into the retailer–ISO bilevel model.

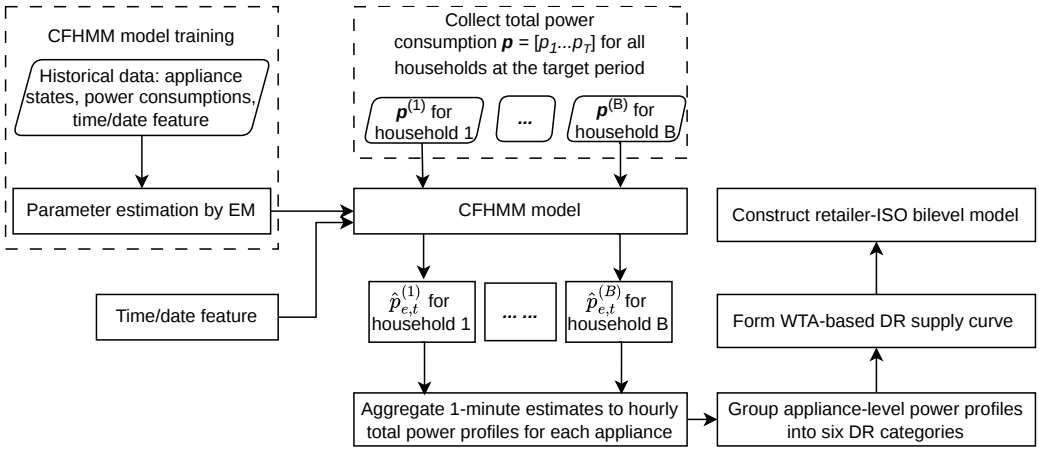


Figure 2. Flowchart of the NILM-based DR incentive design formulation.

3. Solving the Bilevel Problem by a Single MILP

To solve the proposed bilevel programming problem, it is reformulated as a single-level mixed-integer linear program (MILP) relaxation. Specifically, the bilinear terms in the upper-level objective are linearized, and the lower-level problem is replaced by its Karush–Kuhn–Tucker (KKT) optimality conditions.

The generation cost function is assumed to be linear:

$$C_i(g_{i,t}) + C_i^r(r_{i,t}) = c_i g_{i,t} + c_i^r r_{i,t} \tag{34}$$

Moreover, $\lambda_{n,t}$ denotes the dual variable associated with the nodal power-balance constraint (27). $\phi_{\ell,t}$ denotes the dual variable associated with the DC power-flow Equation (28); $\mu_{\ell,t}^+$ and $\mu_{\ell,t}^-$ denote the dual variables of the upper and lower line-flow limits in (29); $\alpha_{i,t}^+$ and $\alpha_{i,t}^-$ denote the dual variables of the upper and lower generator-output limits in (30); γ_t denotes the dual variable of the reserve requirement (31); $\rho_{i,t}^+$ and $\rho_{i,t}^-$ denote the dual variables associated with the reserve-capacity coupling constraint and the reserve non-negativity constraint in (32); and σ_t denotes the dual variable of the reference-bus angle constraint (33).

The Lagrangian for period t is

$$\begin{aligned}\mathcal{L}_t = &\sum_i c_i g_{i,t} + \sum_i c_i^r r_{i,t} + \sum_n \lambda_{n,t}(d_{n,t} - q_{n,t} - \sum_{i\in\mathcal{G}(n)} g_{i,t} + \sum_{\ell\in\delta(n)} f_{\ell,t}) + \sum_\ell \phi_{\ell,t}(f_{\ell,t} \\ &- b_\ell \sum_n A_{\ell,n}\theta_{n,t}) + \sum_\ell \mu_{\ell,t}^+(f_{\ell,t} - F_\ell^{\max}) + \sum_\ell \mu_{\ell,t}^-(-f_{\ell,t} - F_\ell^{\max}) + \sum_i \alpha_{i,t}^+(g_{i,t} - G_i^{\max}) + \sigma_t\theta_{n_0,t} \\ &+ \alpha_{i,t}^-(-g_{i,t} + G_i^{\min}) + \gamma_t(R_t^{\text{req}} - \sum_{i\in\mathcal{G}} r_{i,t}) + \sum_i \rho_{i,t}^-(-r_{i,t}) + \sum_i \rho_{i,t}^+(r_{i,t} + g_{i,t} - G_i^{max})\end{aligned} \tag{35}$$

The stationarity or dual feasibility conditions are

$$c_i - \lambda_{n(i),t} + \alpha^+_{i,t} - \alpha^-_{i,t} + \rho^+_{i,t} = 0, \quad \forall i, t, \tag{36}$$

$$-\sum_{n\in\mathcal{N}} A_{\ell n}\,\lambda_{n,t} + \phi_{\ell,t} + \mu^+_{\ell,t} - \mu^-_{\ell,t} = 0, \quad \forall \ell, t, \tag{37}$$

$$-\sum_{\ell\in\mathcal{L}} A_{\ell n}\,b_\ell\,\phi_{\ell,t} + \sigma_t\,\mathbf{1}\{n = n_0\} = 0, \quad \forall n, t, \tag{38}$$

$$c^r_i - \gamma_t - \rho^-_{i,t} + \rho^+_{i,t} = 0 \quad \forall i, t. \tag{39}$$

$$\mu^+_{\ell,t}, \mu^-_{\ell,t}, \alpha^+_{i,t}, \alpha^-_{i,t}, \gamma_t, \rho^+_{i,t}, \rho^-_{i,t} \geq 0 \tag{40}$$

The complementary slackness conditions are

$$0 \leq \mu^+_{\ell,t} \perp F^{\max}_\ell - f_{\ell,t} \geq 0 \tag{41}$$

$$0 \leq \mu^-_{\ell,t} \perp F^{\max}_\ell + f_{\ell,t} \geq 0 \tag{42}$$

$$0 \leq \alpha^+_{i,t} \perp G^{\max}_i - g_{i,t} \geq 0 \tag{43}$$

$$0 \leq \alpha^-_{i,t} \perp g_{i,t} - G^{\min}_i \geq 0 \tag{44}$$

$$0 \leq \gamma_t \perp \sum_i r_{i,t} - R^{\text{req}}_t \geq 0 \tag{45}$$

$$0 \leq \rho^-_{i,t} \perp r_{i,t} \geq 0 \tag{46}$$

$$0 \leq \rho^+_{i,t} \perp -r_{i,t} - g_{i,t} + G^{max}_i \geq 0 \tag{47}$$

These constraints are linearized using the Big-M method. Here, M is a sufficiently large positive constant, and $u_{1,\ell,t}$, $u_{2,\ell,t}$, $u_{3,i,t}$, $u_{4,i,t}$, $u_{5,t}$, $u_{6,i,t}$, and $u_{7,i,t}$ are binary variables introduced to linearize the corresponding complementarity conditions:

$$\mu^+_{\ell,t} \leq M u_{1,\ell,t}, \qquad F^{\max}_\ell - f_{\ell,t} \leq M(1 - u_{1,\ell,t}) \tag{48}$$

$$\mu^-_{\ell,t} \leq M u_{2,\ell,t}, \qquad F^{\max}_\ell + f_{\ell,t} \leq M(1 - u_{2,\ell,t}) \tag{49}$$

$$\alpha^+_{i,t} \leq M u_{3,i,t}, \qquad G^{\max}_i - g_{i,t} \leq M(1 - u_{3,i,t}) \tag{50}$$

$$\alpha^-_{i,t} \leq M u_{4,i,t}, \qquad g_{i,t} - G^{\min}_i \leq M(1 - u_{4,i,t}) \tag{51}$$

$$\gamma_t \leq M u_{5,t}, \qquad \sum_i r_{i,t} - R^{\text{req}}_t \leq M(1 - u_{5,t}) \tag{52}$$

$$\rho^-_{i,t} \leq M u_{6,i,t}, \qquad r_{i,t} \leq M(1 - u_{6,i,t}) \tag{53}$$

$$\rho^+_{i,t} \leq M u_{7,i,t}, \qquad -r_{i,t} - g_{i,t} + G^{max}_i \leq M(1 - u_{7,i,t}) \tag{54}$$

The objective function of the upper problem has bilinear terms $\tau_t q_{n,t}$ and $\lambda_{n,t} y_{n,t}$. This makes the problem nonconvex and nonlinear and difficult to solve.

First, the bilinear term $\tau_t q_{n,t}$ is linearized using the McCormick envelope [30]. An auxiliary decision variable $w_{n,t} = \tau_t q_{n,t}$ is introduced, with bounds $0 \leq q_{n,t} \leq \bar{q}$ and $\underline{\tau} \leq \tau_t \leq \bar{\tau}$. Then, the bilinear term in the objective function is replaced by $w_{n,t}$, and the four linear inequalities are added. Here, $w_{n,t}$ denotes the auxiliary variable representing the product of the incentive price and the activated DR quantity, $\bar{q}$ denotes the upper bound of activated DR, and $\underline{\tau}$ and $\bar{\tau}$ denote the lower and upper bounds of the incentive price, respectively.

$$w_{n,t} \geq \underline{\tau} q_{n,t}, \tag{55}$$
$$w_{n,t} \geq \bar{q}\tau_t + \bar{\tau} q_{n,t} - \bar{q}\bar{\tau}, \tag{56}$$
$$w_{n,t} \leq \bar{q}\tau_t + \underline{\tau} q_{n,t} - \bar{q}\underline{\tau}, \tag{57}$$
$$w_{n,t} \leq \bar{\tau} q_{n,t}. \tag{58}$$

Then, substituting (20) into the upper-level objective yields

$$\sum_{t\in T}\sum_{n\in N^{DR}} (\pi_t - \lambda_{n,t})(d_{n,t} - q_{n,t}) - \tau_t q_{n,t}. \tag{59}$$

The term $\lambda_{n,t}q_{n,t}$ is eliminated using the strong duality condition of the lower-level linear program. Specifically, for each time period t,

$$\begin{aligned}\sum_{n\in N} \lambda_{n,t} q_{n,t} - \sum_{n\in N} \lambda_{n,t} d_{n,t} = &- \sum_{i\in G} c_i g_{i,t} - \sum_{i\in G} c_i^r r_{i,t} - \sum_{\ell\in L} (\mu_{\ell,t}^+ + \mu_{\ell,t}^-) F_\ell^{\max} \\ &- \sum_{i\in G} \alpha_{i,t}^+ G_i^{\max} + \sum_{i\in G} \alpha_{i,t}^- G_i^{\min} + \rho_{i,t}^+ G_i^{max} + \gamma_t R_t^{req}.\end{aligned} \tag{60}$$

Therefore, the upper-level objective can be rewritten as the following linear expression:

$$\begin{aligned}\max \sum_{t\in T} \Bigg[&\sum_{n\in N^{DR}} \pi_t d_{n,t} - \sum_{n\in N^{DR}} \pi_t q_{n,t} + \sum_{n\in N\setminus N^{DR}} \lambda_{n,t} d_{n,t} - \sum_{i\in G} c_i g_{i,t} - \sum_{i\in G} c_i^r r_{i,t} \\ &- \sum_{\ell\in L} (\mu_{\ell,t}^+ + \mu_{\ell,t}^-) F_\ell^{\max} - \sum_{i\in G} \alpha_{i,t}^+ G_i^{\max} + \sum_{i\in G} \alpha_{i,t}^- G_i^{\min} + \gamma_t R_t^{req} - \sum_{n\in N^{DR}} w_{n,t} \Bigg].\end{aligned} \tag{61}$$

As a result, after including the lower-level primal feasibility conditions, stationarity conditions, and the linearized complementarity constraints, the overall reformulation is a mixed-integer linear program relaxation. The final MILP formulation is summarized in Table 2.

Table 2. MILP reformulation for the proposed bilevel problem.

MILP Reformulation	
variables:	$\tau_t, q_{n,t}, w_{n,t}, b_{n,t,m}, z_{n,t,m}$;
	$g_{i,t}, r_{i,t}, \theta_{n,t}, f_{\ell,t}$;
	$\lambda_{n,t}, \phi_{\ell,t}, \mu_{\ell,t}^+, \mu_{\ell,t}^-, \alpha_{i,t}^+, \alpha_{i,t}^-, \gamma_t, \sigma_t, \rho_{i,t}^+, \rho_{i,t}^-$
	$u_{1,\ell,t}, u_{2,\ell,t}, u_{3,i,t}, u_{4,i,t}, u_{5,t}, u_{6,i,t}, u_{7,i,t} \in \{0,1\}$
maximize:	(61)
subject to:	(15)–(25) and (55)–(58),(27)–(33),(36)–(40),(48)–(54)

In summary, the reformulation of the bilevel model follows the procedure shown in Figure 3. The retailer–ISO bilevel model is first decomposed into upper-level and lower-level problems. The ISO market-clearing problem is reformulated through KKT conditions and the resulting complementarity conditions are linearized using the Big-M method. Meanwhile, the bilinear incentive-payment terms in the upper-level problem are linearized using the McCormick method. The lower-level reformulation and upper-level linearization are then combined into a single-level MILP formulation, from which the optimal incentive and market results are obtained.

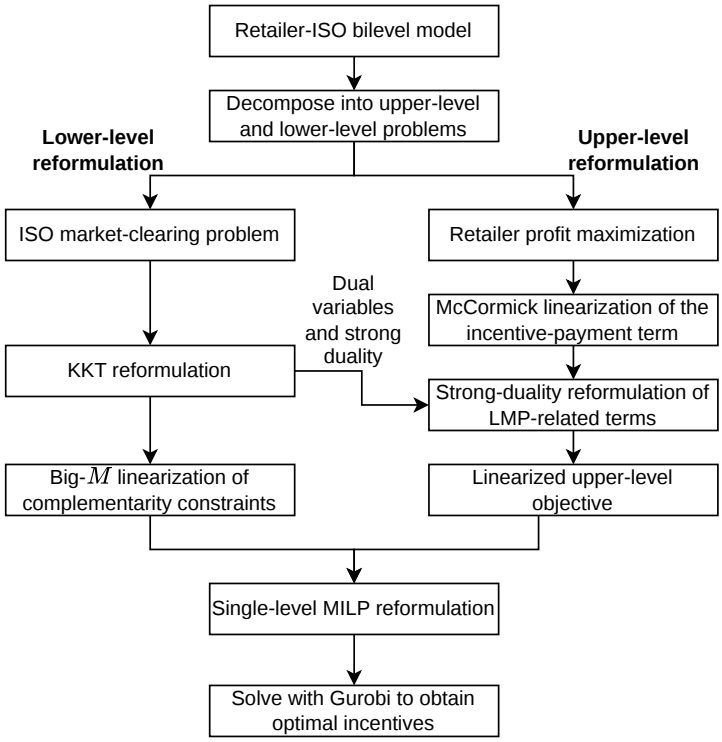


Figure 3. Flowchart of the single-level MILP reformulation procedure.

4. Case Study

The proposed framework is evaluated on a modified IEEE 30-bus system over a 24-h horizon. Retail demand is assigned to buses 7, 15, and 30, with hourly variation introduced through a normalized load profile. The modified IEEE 30-bus system used for the case study is illustrated in Figure 4. Buses 7, 15, and 30 are selected as DR aggregation buses, where the retailer-side flexible loads are connected and participate in the incentive-based demand response program.

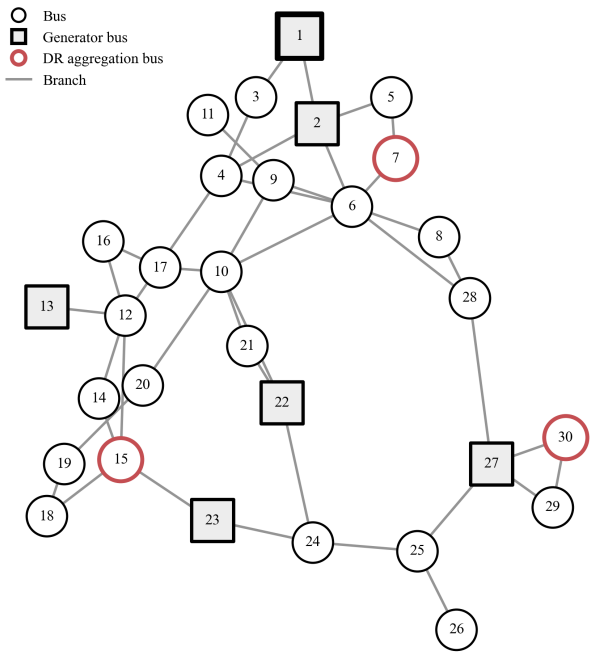


Figure 4. Schematic diagram of the modified IEEE 30-bus system. Numbers denote bus indices and red circles represent DR aggregation buses.

Smart-meter data from the Pecan Street dataset [31] are used to construct appliance-level consumption profiles. The dataset consists of residential electricity measurements organized by buildings and meter channels. The dataset provides time-indexed active-power measurements, including both aggregate household load and submetered appliance-level electricity data. The raw smart-meter measurements have a discrete recording step of 1 min. Potential data-quality issues include missing or empty records, duplicate timestamps, timestamp misalignment among different meter channels, measurement noise, abnormal readings, and communication-related data gaps. Therefore, empty records are removed, duplicate timestamps are filtered, and different meter channels are time-aligned.

Three scenarios are considered: (1) no DR, where no demand response is available; (2) aggregate DR, where DR is represented by a single aggregate segment with a uniform willingness-to-accept threshold; and (3) NILM-based DR, where flexible loads are extracted from NILM results and represented by time-varying segment-wise WTA curves. Simulations are conducted on an Intel Core i7-13850HX computer with a 2.10 GHz CPU, 64 GB RAM, and a 64-bit Windows operating system.

4.1. Nilm-Based DR Potential Extraction

The CFHMM is trained using smart-meter data from 1 January to 24 January 2018, and evaluated on the following one-week test period from 25 January to 31 January 2018. The disaggregation results are compared across six appliance categories, including HVAC, EV charging, washer/dryer, dishwasher, lighting, and others. Table 3 reports the root mean square error (RMSE) and mean absolute error (MAE) over the one-week test set. In addition, Figure 5 shows the one-day true and estimated consumption profiles for two representative flexible appliance categories on the selected representative day. The results indicate that the CFHMM captures the main temporal patterns of major flexible loads, such as EV charging and washer/dryer, although discrepancies remain for intermittent loads. These disaggregated profiles are then used to construct appliance-level DR potential inputs for the subsequent optimization model.

Table 3. NILM performance by appliance category on the one-week test set.

Appliance	RMSE (kWh)	MAE (kWh)
HVAC	0.4034	0.3279
EV	0.8157	0.4219
Washer/Dryer	0.7071	0.3876
Dishwasher	0.1752	0.1276
Lighting	0.4977	0.3835
Others	0.2577	0.2034

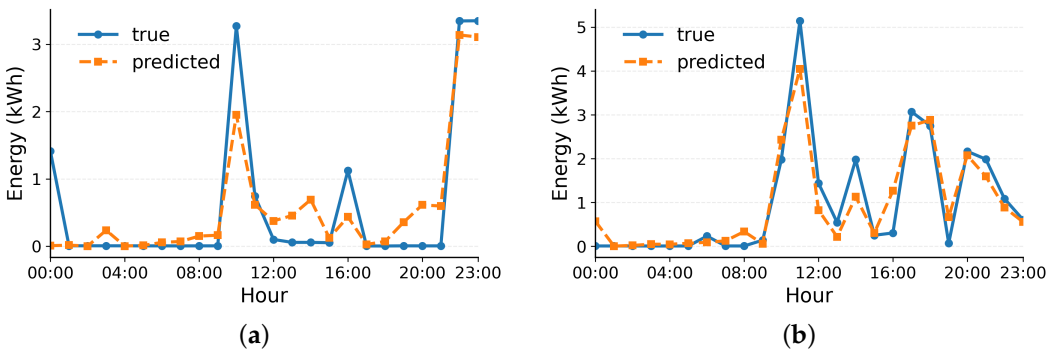


Figure 5. One-day NILM disaggregation results for representative flexible loads. (**a**) EV. (**b**) Washer/Dryer.

Based on the disaggregated profiles, stepwise DR supply functions are constructed for each time period. WTA values are assigned exogenously based on empirical evidence from

prior studies [15,16], reflecting the heterogeneity of user inconvenience across end uses. For the base-case illustration, the WTA vector is set as $[v_0, \ldots, v_5] = [5, 10, 15, 20, 25, 1000]$ in \$/MWh. v_5 is a large number so the base load cannot be activated. These values are not intended to represent universal compensation estimates; rather, they encode a representative ordering of appliance flexibility costs for the numerical experiment.

The proposed optimization framework is separate from the process by which WTA parameters are obtained. In practical implementations, WTA values may be estimated from surveys, choice experiments, historical DR participation, randomized incentive trials, or inverse optimization using observed customer responses. The system-level integration of NILM-derived flexibility into incentive design is the focus of this study, while the empirical estimation of customer-specific WTA is left for future work.

Figure 6 illustrates the resulting DR supply curves at four representative hours ($t = 4, 10, 15, 19$). Two observations follow directly from these curves: (1) multiple WTA tiers indicate within-hour heterogeneity in flexibility cost, and (2) the total available flexible quantity varies across hours, reflecting the time-varying availability of end-use loads. In contrast, the aggregate DR scenario collapses this structure into a single segment, thereby losing both heterogeneity and temporal detail.

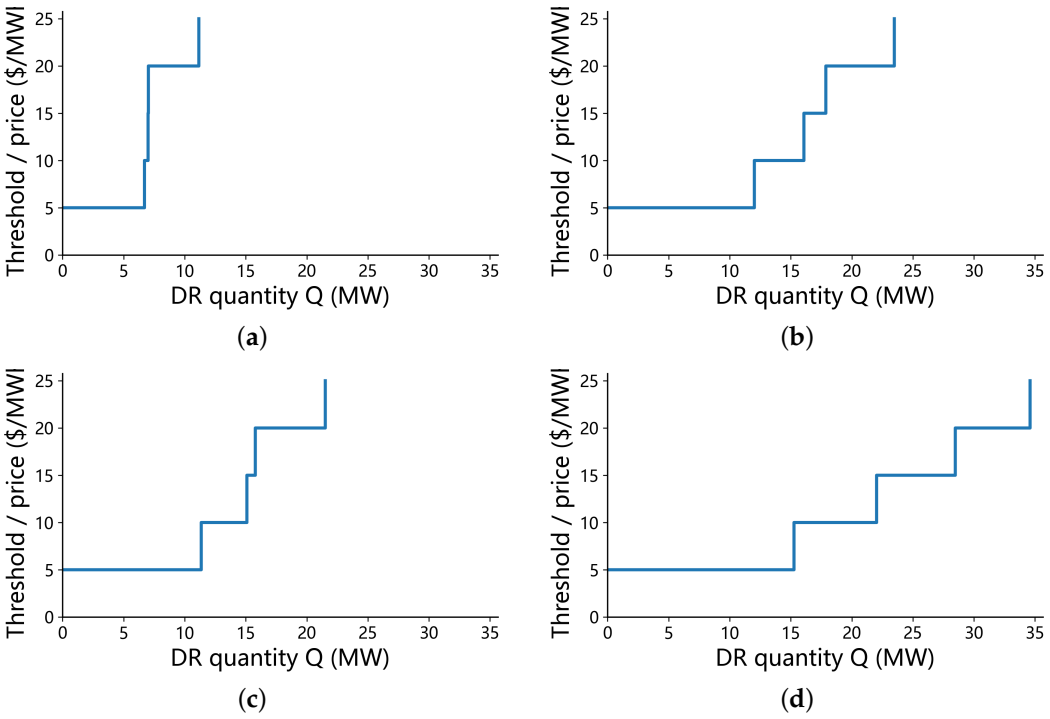


Figure 6. Stepwise DR supply curves under the appliance-informed setting (NILM-based DR) at representative hours. (**a**) $t = 4$. (**b**) $t = 10$. (**c**) $t = 15$. (**d**) $t = 19$.

4.2. Optimal Incentive Strategies

Using the derived DR supply curves, the retailer optimizes hourly incentives within the bilevel framework. The retailer determines incentive levels and procured DR quantities, while the ISO clears the market via DC optimal power flow, producing LMPs.

Table 4 compares the objective values and economic metrics across scenarios. Compared with the no-DR case, aggregate DR improves the retailer's objective value from 11,871.2328 to 12,041.0514 while reducing the energy cost from 23,411.9672 to 22,940.8336. Under the NILM-based DR representation, the objective value further increases to 12,284.3928, the activated DR rises to 9.7405 MWh, and the energy cost decreases to 22,389.6860.

Table 4. Optimal objective values under the three case-study scenarios.

Scenario	Objective Value ($)	DR Activated (MWh)	Energy Cost ($)
No DR	11,871.2328	0.0000	23,411.9672
Aggregate DR	12,041.0514	3.6412	22,940.8336
NILM-based DR	12,284.3928	9.7405	22,389.6860

Figure 7 further illustrates bus-level DR activation patterns under the two active DR scenarios. In aggregate DR, activation is limited. In NILM-based DR, activation becomes time-varying and spatially differentiated, reflecting both network conditions and heterogeneous flexibility availability. The stacked bars show the contribution of each DR bus to the total activated response at each time period. The corresponding incentive signals are reflected in the optimized DR activation and price responses.

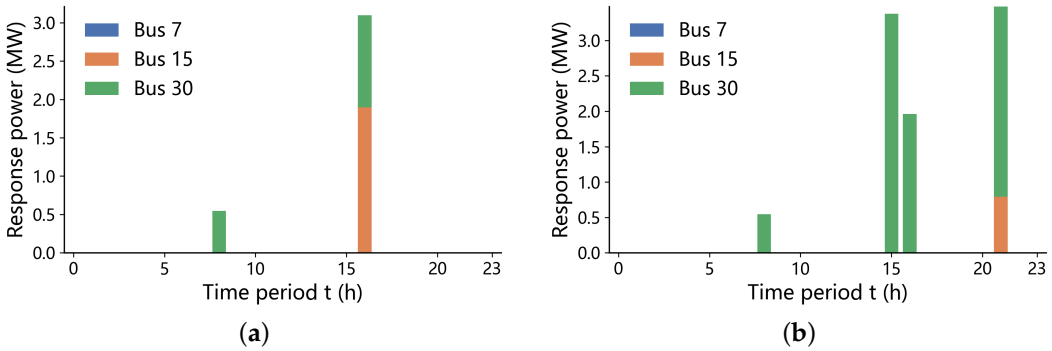


Figure 7. Bus-level DR activation at buses 7, 15, and 30 under the two active DR scenarios. Each bar is stacked by the activated DR contributions from the three buses. The no-DR case is omitted because DR activation is identically zero for all buses and hours. (**a**) Aggregate DR. (**b**) NILM-based DR.

Figure 8 compares the LMP trajectories for each bus–scenario pair. At bus 7, where the activated DR quantity is limited, the LMP profiles are nearly identical across scenarios, suggesting that DR has only a marginal impact on the local market-clearing price. In contrast, at bus 15, where a moderate amount of flexible demand is available, the NILM-based DR representation produces larger and more temporally concentrated LMP reductions, especially during hours with high flexible-load availability and binding network conditions. The effect is also evident at bus 30, where the interaction between local DR activation and network constraints leads to more visible price deviations from the no-DR benchmark. These observations demonstrate that appliance-informed flexibility changes not only the amount of DR activated, but also the timing and location of its market impacts.

4.3. Sensitivity Analysis

As WTA increases, fewer DR segments satisfy the activation condition, reducing total activated DR, as shown in Figure 9. Incentive payments may change non-monotonically because they depend jointly on the activated quantity and the marginal WTA level of selected segments. Overall, higher WTA values reduce the retailer's objective value, although the effect is relatively modest in the tested range. In the base case, the objective value is 12,282. When all WTA values are reduced by 20%, the objective value increases to 12,302 because more low-cost flexibility becomes available, whereas increasing all WTA values by 20% lowers the objective value to 12,259 due to reduced DR participation and higher compensation requirements.

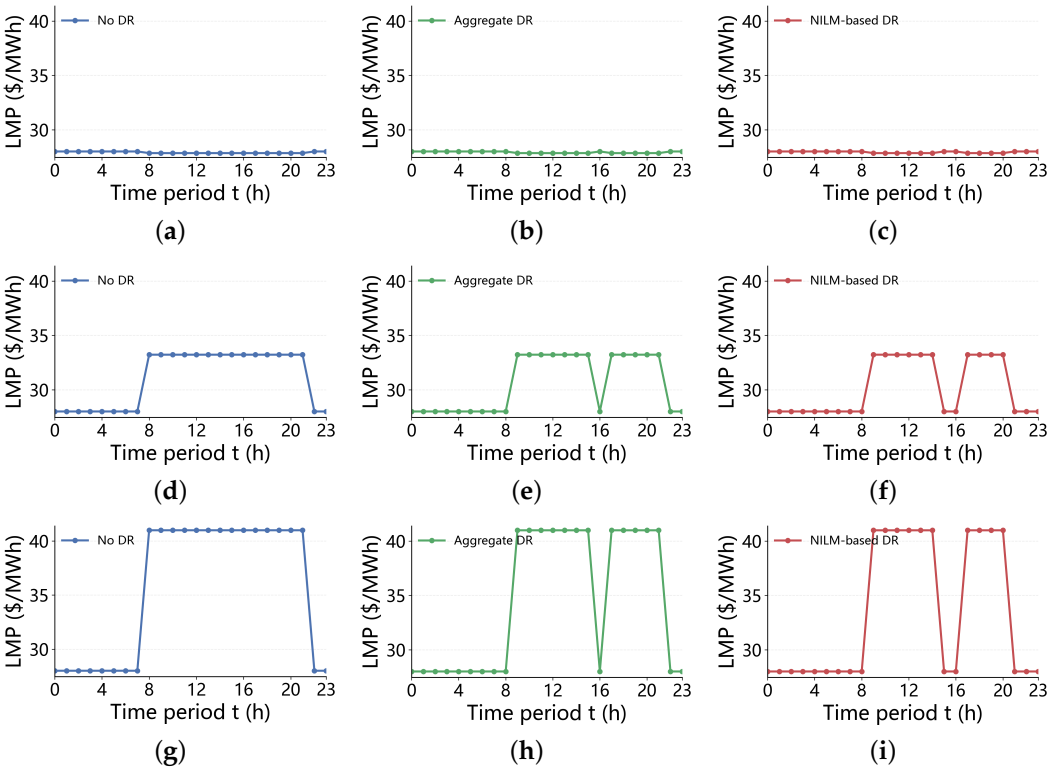


Figure 8. LMP trajectories at buses 7, 15, and 30 under the three scenarios. (**a**) Bus 7, no DR. (**b**) Bus 7, aggregate DR. (**c**) Bus 7, NILM-based DR. (**d**) Bus 15, no DR. (**e**) Bus 15, aggregate DR. (**f**) Bus 15, NILM-based DR. (**g**) Bus 30, no DR. (**h**) Bus 30, aggregate DR. (**i**) Bus 30, NILM-based DR.

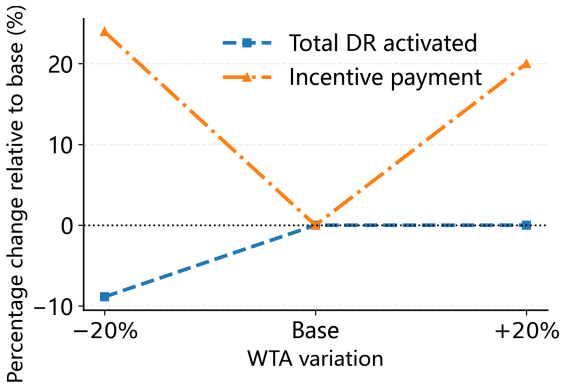


Figure 9. Percentage changes in total DR activation and incentive payment relative to the base case.

To evaluate the dependency on disaggregation accuracy, the optimization model is run using ground-truth appliance profiles and CFHMM-estimated profiles. Table 5 compares the resulting objective value, total activated DR, and maximum hourly DR activation. It shows that the disaggregation error affects the quantity of the activated DR.

Table 5. Impact of NILM accuracy on optimization results.

Input Data	Objective Value ($)	DR Activated (MWh)	Maximum Hourly DR (MW)
Ground truth	12,326.7957	15.3246	5.6682
CFHMM output	12,284.3928	9.7405	3.8533

To quantify this impact, an additional sensitivity test is conducted by perturbing the estimated flexible load by −10%, −5%, +5%, and +10%, while adjusting the inflexible base load accordingly to keep the total demand profile consistent. As shown in Figure 10, the LMP deviations remain close to zero for most time periods; bus 7 shows only minor

deviations, while buses 15 and 30 exhibit more visible deviations at a few sensitive hours, especially under ±10% perturbations. These results indicate that discrepancies in estimating flexible-load usage profiles may affect LMP trajectories when the system operates near a marginal or network-constrained condition, while the overall impact remains localized in time and location.

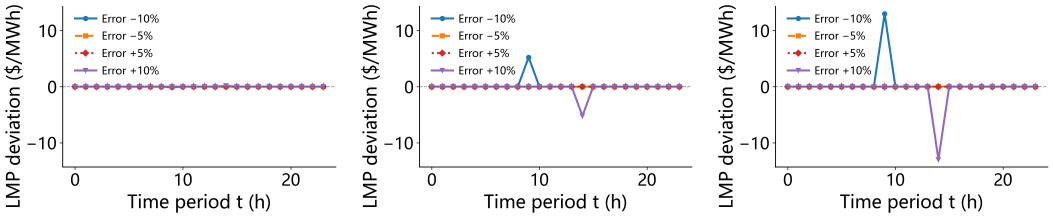


Figure 10. LMP deviations caused by flexible-load profile perturbations at buses 7, 15, and 30. (**a**) Bus 7. (**b**) Bus 15. (**c**) Bus 30.

Finally, Table 6 reports the solver statistics for the three scenarios. The model size increases from the no-DR case to the aggregate DR case and further to the NILM-based DR case, reflecting the additional variables and constraints introduced by the increasingly detailed DR representation.

Table 6. MILP performance metrics.

Scenario	Solve Time (s)	MIP Gap (%)	Variables	Constraints
No DR	1.8169	0.0	9288	11,951
Aggregate DR	1.1686	0.0	9384	12,311
NILM-based DR	2.3617	0.0	10,344	14,039

The zero mixed-integer programming (MIP) gaps reported in Table 6 indicate that the MILP solver converged to proven optimal solutions within the solver tolerance for all three scenarios.

5. Conclusions

A bilevel programming framework is proposed for DR incentive design by integrating appliance-level flexibility derived from NILM. A CFHMM-based NILM method is used to recover appliance-level consumption patterns from low-frequency electricity measurements. By mapping disaggregated end-use consumption to stepwise WTA functions, the framework captures both the heterogeneity and temporal variability of demand-side flexibility. The resulting DR representation is embedded into a retailer–ISO bilevel model, where incentive decisions and market-clearing outcomes are jointly determined. The bilevel model is reformulated as a single-level MILP by applying KKT conditions to the lower-level market-clearing problem and linearizing the resulting complementarity and bilinear terms.

The case study on a modified IEEE 30-bus system and real smart meter data demonstrates the effectiveness of the proposed framework. Compared with the no-DR and aggregate DR cases, the NILM-based DR representation enables more detailed identification of flexible demand and leads to improved retailer economic performance. The results show that appliance-informed flexibility increases the total activated DR quantity and reduces energy procurement costs. Sensitivity analyses indicate that the proposed model responds consistently to changes in WTA values and NILM accuracy, confirming the relevance of both customer compensation assumptions and disaggregation quality to the final incentive strategy. These results highlight the importance of representing demand

flexibility with sufficient granularity, as coarse aggregate models may underestimate both the value and operational impact of DR.

Future research can extend this work in several directions. First, more advanced NILM methods can be integrated to improve the estimation of flexible loads, especially for intermittent and multi-mode appliances. Second, future work may consider practical implementation issues, such as customer privacy, communication requirements, incentive settlement, and the integration of the proposed framework into real-world DR programs.

Author Contributions: Conceptualization, K.Z.; methodology, K.Z.; formal analysis, Y.D.; investigation, Y.D.; resources, X.H.; writing—original draft, Y.D. and K.Z.; writing—review and editing, X.H. and Y.S.; funding acquisition, K.Z.; supervision, Y.S.; project administration, Y.S. All authors have read and agreed to the published version of the manuscript.

Funding: This research was supported in part by the National Natural Science Foundation of China under Grant 52407132, in part by Collaborative Innovation Center of Industrial Energy-saving and Power Quality Control under Grant KFKT202509, and in part by China Postdoctoral Science Foundation under 2025M770509.

Data Availability Statement: The data presented in this study are partially available from publicly accessible sources, as cited in the paper. Additional data are available from the corresponding author upon request.

Conflicts of Interest: Author X.H. was employed by Suzhou Electrical Apparatus Science Research Institute Co., Ltd. during the conduction of this study. All authors declare that the research was conducted in the absence of any commercial or financial relationships that could be construed as potential conflicts of interest.

Nomenclature

Sets

$t \in \mathcal{T}$	Time periods.
$n \in \mathcal{N}, \mathcal{N}^{\mathrm{DR}}$	Buses and DR buses.
$\delta(n)$	Set of lines incident to bus n.
$i \in \mathcal{G}(n)$	Generators at bus n.
$\mathcal{G} = \cup_n \mathcal{G}(n)$	Set of all generators.
$\ell \in \mathcal{L}$	Transmission lines.
$m \in \mathcal{M}$	DR availability segments.

Parameters

$d_{n,t}$	Baseline (pre-DR) demand at bus n (MWh).
$h_{n,t,m}$	Available capacity of DR segment m at bus n and time t.
π_t	Exogenous end-user retail tariff (USD/MWh).
$C_i(g)$	Generation cost function.
$C_i^r(r_{i,t})$	Reserve cost function of generator i.
$G_i^{\min}$, $G_i^{\max}$	Minimum and maximum generation limits.
b_ℓ	Line susceptance for line ℓ.
$A_{\ell n}$	Line-bus incidence matrix element.
$F_\ell^{\max}$	Line thermal flow limit.
n_0	Slack bus.
v_m	Willingness-to-accept threshold of DR segment m (USD/MWh).
$\underline{\tau}, \bar{\tau}$	Lower and upper bounds of the DR incentive price (USD/MWh).
$R^{\mathrm{up}}, R^{\mathrm{down}}$	Upward and downward ramp limits for DR activation.
$E_{\max}^{DR}$	Upper limit for DR activation.
R_t^{req}	Total generation reserve requirement.

Variables

$q_{n,t}$	Activated DR capacity at bus n and time t.
$b_{n,t,m}$	Activated DR capacity segment m at bus n and time t.
$z_{n,t,m}$	Activation status of DR capacity segment m at bus n and time t.
τ_t	Incentive price (USD/MWh) at time t.
$g_{i,t}$	Generation dispatch for generator i at time t.
$r_{i,t}$	Generation reserve for generator i at time t.
$y_{n,t}$	Post-DR served retail demand at bus n and time t.
$\lambda_{n,t}$	Locational marginal price at bus n and time t.
$\theta_{n,t}$	Voltage angle at bus n.
$f_{\ell,t}$	Power flow on line ℓ.

References

1. Pratt, A.; Krishnamurthy, D.; Ruth, M.; Wu, H.; Lunacek, M.; Vaynshenk, P. Transactive Home Energy Management Systems: The Impact of Their Proliferation on the Electric Grid. *IEEE Electrif. Mag.* **2016**, *4*, 8–14. [CrossRef]
2. Faruqui, A.; Sergici, S. Household Response to Dynamic Pricing of Electricity: A Survey of 15 Experiments. *J. Regul. Econ.* **2010**, *38*, 193–225. [CrossRef]
3. Dupont, B.; Dietrich, K.; De Jonghe, C.; Ramos, A.; Belmans, R. Impact of residential demand response on power system operation: A Belgian case study. *Appl. Energy* **2014**, *122*, 1–10. [CrossRef]
4. Lau, E.T.; Yang, Q.; Stokes, L.; Taylor, G.A.; Forbes, A.B.; Clarkson, P.; Wright, P.S.; Livina, V.N. Carbon savings in the UK demand side response programmes. *Appl. Energy* **2015**, *159*, 478–489. [CrossRef]
5. Albadi, M.H.; El-Saadany, E.F. A Summary of Demand Response in Electricity Markets. *Electr. Power Syst. Res.* **2008**, *78*, 1989–1996. [CrossRef]
6. Mohsenian-Rad, A.H.; Wong, V.W.S.; Jatskevich, J.; Schober, R.; Leon-Garcia, A. Autonomous Demand-Side Management Based on Game-Theoretic Energy Consumption Scheduling for the Future Smart Grid. *IEEE Trans. Smart Grid* **2010**, *1*, 320–331. [CrossRef]
7. Hogan, W.W. Contract Networks for Electric Power Transmission. *J. Regul. Econ.* **1992**, *4*, 211–242. [CrossRef]
8. Huang, H.; Miao, P.; Wei, Q.; Geng, Y. Bilevel Optimization in Smart Grid Operations: A Review of Real-Time Electricity Pricing Strategies and Future Directions. *Electr. Power Syst. Res.* **2026**, *251*, 112253. [CrossRef]
9. Liu, S.; Yang, R.; Liu, Y. New Distributionally Robust Optimization Framework and Algorithm for Energy Hub Scheduling Integrating Demand Response Programs under Ambiguous Prices and Loads. *Appl. Energy* **2026**, *405*, 127211. [CrossRef]
10. Zugno, M.; Morales, J.M.; Pinson, P.; Madsen, H. A Bilevel Model for Electricity Retailers' Participation in a Demand Response Market Environment. *Energy Econ.* **2013**, *36*, 182–197. [CrossRef]
11. Ruiz, C.; Conejo, A. Pool Strategy of a Producer with Endogenous Formation of Locational Marginal Prices. *IEEE Trans. Power Syst.* **2009**, *24*, 1855–1866. [CrossRef]
12. Anwar, M.B.; O'Malley, M. Strategic Participation of Residential Thermal Demand Response in Energy and Capacity Markets. *IEEE Trans. Smart Grid* **2021**, *12*, 3070–3085. [CrossRef]
13. Qiu, D.; Wang, Y.; Wang, J.; Jiang, C.; Strbac, G. Personalized Retail Pricing Design for Smart Metering Consumers in Electricity Market. *Appl. Energy* **2023**, *348*, 121545. [CrossRef]
14. Ma, L.; Liu, S.; Liu, J. Distributionally Robust Optimal Bidding of Energy Hubs in the Joint Electricity and Carbon Market. *Front. Energy Res.* **2022**, *10*, 898620. [CrossRef]
15. Xu, S.; Yang, Z.; Deng, N.; Wang, B. Residents' Willingness to Be Compensated for Power Rationing during Peak Hours Based on Choice Experiment. *Appl. Energy* **2024**, *367*, 123335. [CrossRef]
16. Ladenburg, J.; Jensen, K.L.; Lodahl, C.; Keles, D. Testing for Non-Linear Willingness to Accept Compensation for Controlled Electricity Switch-Offs Using Choice Experiments. *Energy* **2022**, *238*, 121749. [CrossRef]
17. Srivastava, A.; Van Passel, S.; Kessels, R.; Valkering, P.; Laes, E. Reducing Winter Peaks in Electricity Consumption: A Choice Experiment to Structure Demand Response Programs. *Energy Policy* **2020**, *137*, 111183. [CrossRef]
18. Wang, A.; Li, R.; You, S. Development of a Data Driven Approach to Explore the Energy Flexibility Potential of Building Clusters. *Appl. Energy* **2018**, *232*, 89–100. [CrossRef]
19. Wan, Y.; Qin, J.; Yu, X.; Yang, T.; Kang, Y. Price-Based Residential Demand Response Management in Smart Grids: A Reinforcement Learning-Based Approach. *IEEE/CAA J. Autom. Sin.* **2022**, *9*, 123–134. [CrossRef]
20. Kovács, A. Inverse Optimization Approach to the Identification of Electricity Consumer Models. *Cent. Eur. J. Oper. Res.* **2021**, *29*, 521–537. [CrossRef]
21. Hart, G. Nonintrusive Appliance Load Monitoring. *Proc. IEEE* **1992**, *80*, 1870–1891. [CrossRef]

22. Huber, P.; Calatroni, A.; Rumsch, A.; Paice, A. Review on Deep Neural Networks Applied to Low-Frequency NILM. *Energies* **2021**, *14*, 2390. [CrossRef]
23. Papageorgiou, P.G.; Christoforidis, G.C.; Bouhouras, A.S. NILM in High Frequency Domain: A Critical Review on Recent Trends and Practical Challenges. *Renew. Sustain. Energy Rev.* **2025**, *213*, 115497. [CrossRef]
24. Lin, J.; Ma, J.; Zhu, J.; Liang, H. Deep Domain Adaptation for Non-Intrusive Load Monitoring Based on a Knowledge Transfer Learning Network. *IEEE Trans. Smart Grid* **2022**, *13*, 280–292. [CrossRef]
25. Gao, A.; Zheng, J.; Mei, F.; Liu, Y. Toward Intelligent Demand-Side Energy Management via Substation-Level Flexible Load Disaggregation. *Appl. Energy* **2024**, *367*, 123361. [CrossRef]
26. Yue, H.; Yan, K.; Zhao, J.; Ren, Y.; Yan, X.; Zhao, H. Estimating Demand Response Flexibility of Smart Home Appliances via NILM Algorithm. In *Proceedings of the 2020 IEEE 4th Information Technology, Networking, Electronic and Automation Control Conference (ITNEC)*; IEEE: Piscataway, NJ, USA, 2020; Volume 1, pp. 394–398.
27. He, D.; Lin, W.; Liu, N.; Harley, R.G.; Habetler, T.G. Incorporating Non-Intrusive Load Monitoring Into Building Level Demand Response. *IEEE Trans. Smart Grid* **2013**, *4*, 1870–1877. [CrossRef]
28. Kim, H.; Marwah, M.; Arlitt, M.; Lyon, G.; Han, J. Unsupervised disaggregation of low frequency power measurements. In *Proceedings of the 2011 SIAM International Conference on Data Mining*; SIAM: Philadelphia, PA, USA, 2011; pp. 747–758.
29. Moon, T.K. The expectation-maximization algorithm. *IEEE Signal Process. Mag.* **1996**, *13*, 47–60. [CrossRef]
30. McCormick, G.P. Computability of global solutions to factorable nonconvex programs: Part I—Convex underestimating problems. *Math. Program.* **1976**, *10*, 147–175. [CrossRef]
31. Smith, C.A. The Pecan Street Project: Developing the Electric Utility System of the Future. Ph.D. Thesis, University of Texas, Austin, TX, USA, 2009.

Disclaimer/Publisher's Note: The statements, opinions and data contained in all publications are solely those of the individual author(s) and contributor(s) and not of MDPI and/or the editor(s). MDPI and/or the editor(s) disclaim responsibility for any injury to people or property resulting from any ideas, methods, instructions or products referred to in the content.